

Two-photon physics at future electron-positron colliders

I.R.Boyko, V.V.Bytev and A.S.Zhemchugov
Joint Institute for Nuclear Research, Dubna, Russia

October 31, 2022

Abstract

Two photon collisions offer a variety of physics studies that can be performed at the future electron-positron colliders. Using the planned CEPC parameters as a benchmark we consider several topics to be studied in the two-photon collisions. With the full integrated luminosity the Higgs boson photoproduction can be reliably observed. A large statistics of various quarkonium states can be collected. The LEP results on the photon structure function and the tau lepton anomalous magnetic moment can be improved by 1-2 orders of magnitude.

1 Introduction

The flagship of the modern particle physics, the LHC, is expected to continue running for more than 10 year from now. However, the planning of the next generation colliders has already started.

It is widely believed that the next major collider project can be a high-energy, high-luminosity electron-positron collider. Currently four mature projects of e^+e^- colliders are under consideration: linear colliders CLIC [1] and ILC [2] and circular colliders CEPC [3] and FCC-ee [4].

The scientific programs of the future e^+e^- colliders are well developed. The main goals are the Higgs boson physics; high-precision measurements at the Z pole energy; the top quark physics; searches for new physics phenomena. In this paper we investigate prospects for another branch of the experimental program: the physics of two photon collisions.

The collisions of (quasi-)virtual photons are responsible for a significant fraction of the total event rate at electron-positron colliders. They are especially abundant at the linear colliders due to high acceleration gradients. Such events represent an unpleasant background for the studies of other physics processes. On the other hand, the two-photon collisions themselves provide opportunities for interesting

physics studies. In this paper we analyze several topics which can be investigated using the two-photon collisions at the future e^+e^- colliders.

At the linear colliders the rate and the energy spectrum of the two-photon collisions depend of the particular configuration of beams. Therefore our study is restricted to the case of circular colliders, where the differential gamma-gamma luminosity can be predicted from the first principles.

Both CEPC and FCC are expected to take large data sets at 240 GeV center-of-mass energy (a point close to the maximum yield of Higgs bosons). The CEPC expected integrated luminosity is 5.6 ab^{-1} . FCC plans to collect at least 5 ab^{-1} at 240 GeV, followed by 1.7 ab^{-1} at the energies of top pair production (340-365 GeV). In this paper we use the CEPC planned energy and luminosity as a benchmark scenario; however, our qualitative results are also applicable to the FCC which has a similar expected performance.

2 Two-photon collisions at electron-positron colliders

The era of two-photon physics had been started in early 1970th, when a relatively high cross section of the 4-th order QED process $e^+e^- \rightarrow e^+e^-e^+e^-$ was observed [5] in Budker Institute of Nuclear Physics (Novosibirsk).

It should be noted that the first theoretical predictions for a photoproduction of pions [6], [7] in e^+e^- collision had been made back around 1960, the calculated cross-sections deemed unmeasurably small and no further elaboration has been done till the late 60th. At that time a series of papers covering multiple final states of e^+e^- colliders had been published, but only after experimental observation at Novosibirsk the most remarkable mechanism of cross-section enhancement due to small virtuality of photons emitted by the electrons was revealed [8].

It is the small virtuality of intermediate photons that features two main characteristics of two-photon processes: enhancement of the yield with the increase of colliding beam energies and the possibility to study new type of processes $\gamma\gamma \rightarrow X$ with two variable parameters - the virtualities of intermediate photons.

The two-photon process can occur at electron-positron or electron-electron colliders:

$$e^\pm + e^- \rightarrow e^\pm + e^- + \gamma^* + \gamma^* \rightarrow e^\pm + e^- + X,$$

where X describes an arbitrary final state. Not any final state can be produced in the two-photon processes: since two photons have even C parity, only states with $C=+1$ are possible. As it was mentioned above, two-photon cross-section slowly rises with the energy and becomes greater than the one of the annihilation channel at $\sqrt{s}/2 \gtrsim 1 \text{ GeV}$.

In a two-photon process the initial particles (electrons and/or positrons) emit two photons with virtualities q_1 and q_2 and the latter merge in some final system of particles X with invariant mass square $W^2 = (q_1 + q_2)^2$, see Fig.2.

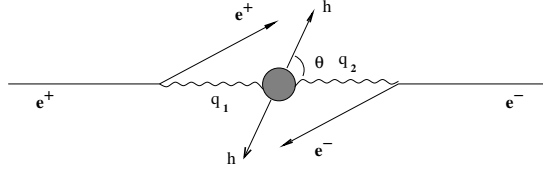


Figure 1: Kinematics of a two-photon process.

The cross-section of two-photon scattering of electron (positron) can be calculated as a convolution of amplitudes describing the emission of virtual photons off initial particle and the $\gamma\gamma \rightarrow X$ transition. The first one is calculated within the QED, and the second can be expanded in independent tensors, the choice of which is quite arbitrary up to the conservation of the Lorentz invariance, T- and gauge invariance. For the sake of physical interpretation, it is encoded in five structure functions. Three of them can be expressed through the cross section $\sigma_{a,b}$ for scalar ($a, b = S$) and transverse photons ($a, b = T$). The other structure functions τ_{TT} and τ_{TS} correspond to transitions with spin-flip for each of the photons with total helicity conservation [9]:

$$d\sigma = \frac{\alpha^2}{16\pi^4 q_1^2 q_2^2} \sqrt{\frac{(q_1 q_2)^2 - q_1^2 q_2^2}{(p_1 p_2)^2 - m_e^2 m_e^2}} \left(4\rho_1^{++} \rho_2^{++} \sigma_{TT} + 2|\rho_1^{+-} \rho_2^{+-}| \tau_{TT} \cos(2\tilde{\phi}) \right. \\ \left. + 2\rho_1^{++} \rho_2^{00} \sigma_{TS} + 2\rho_1^{00} \rho_2^{++} \sigma_{ST} + \rho_1^{00} \rho_2^{00} \sigma_{SS} - 8|\rho_1^{+0} \rho_2^{+0}| \tau_{TS} \cos(\tilde{\phi}) \right) \frac{d^3 p'_1 d^3 p'_2}{E_1 E_2}, \quad (1)$$

where ρ_i^{ab} are the density matrices of the virtual photon in the $\gamma\gamma$ -helicity basis, $p_i, (p'_i)$ corresponds to the momentum and energy of initial (scattered) leptons, E_i stands for scattered lepton energies, $\tilde{\phi}$ is the angle between the scattering planes of colliding particles in c.m.s. of photons, m_e is the mass of the initial lepton.

The exact formula (1) provides an accurate estimation of two-photon process at any kinematical region and could be used for quantitatively correct simulations [10, 11]. At the limit $q_i^2 \rightarrow 0$ one can see a logarithmic enhancement of cross-section, with natural kinematic "regularization" value at m_e^2 .

The small q_i^2 domain gives the main contribution to the cross-section of the process under consideration. In this limit the expression for (1) can be simplified under the procedure called Equivalent Photon Approximation (Weizacher-Williams' method).

Keeping in mind this approximation and taking into account only leading terms we can see that the cross-section of the two-photon process factorizes into two different parts: one part is connected with emission of two real photon by initial particles and the other is the final state production by the two photons [12]:

$$\frac{d\sigma^{(0)}}{dW^2 d\Gamma} = 2 \left(\frac{\alpha}{\pi} \right)^2 \frac{1}{W^2} \ln^2 \frac{E}{m_e} f\left(\frac{W}{2E}\right) \frac{d\sigma_{\gamma\gamma \rightarrow X}(W^2)}{d\Gamma}, \quad (2)$$

where E is the energy of the initial particle and

$$f(\gamma) = -(2 + \gamma^2)^2 \ln \gamma - (1 - \gamma^2)(3 + \gamma^2) \quad (3)$$

is the factor describing the luminosity dependence over the invariant mass of the colliding photons, Γ stands for phase volume of final state X .

The cost of this simplicity is the underestimation of cross-section in some specific kinematics, the loss of the information on the initial particle scattering angle and missing deep virtual scattering behaviour of cross-section, when one of the photon has a rather large invariant mass. Of course, events with big virtuality of an intermediate photon are much more rare, since there is no q_i^2 pole enhancement.

Small q_i^2 invariant mass of emitted photons means that the scattered leptons proceed undetected (so called no-tag events), but due to large cross-section of the process the no-tag events can be selected even without full final state recovery [13], using the requirements of the small total transverse momentum of the produced system and small value of its invariant mass ($W \ll 2E$). The gamma-gamma collisions tend to occur at the c.m.s. energies much less than the nominal collider energy, as can be seen in Fig. 2 (left). Nevertheless, the amount of collisions at rather high energies is also significant and can be used to study different aspects of the two-photon physics.

Practically, one can tag two photon events by detection of one or both scattered electrons (single tag or double tag mode). Tagging allows one to suppress background significantly at the cost of steep reduction of available statistics. In this case the requirement of tagging the lepton(s) in a given energy and angular range means non-vanishing virtualities of photon mass and gives one the possibility to measure the q_i^2 dependence of the two-photon cross-section (1). In this paper we suppose that scattered particles can be tagged in the luminosity monitor. A typical CEPC and FCC-ee acceptance down to 30 mrad is assumed.

The two-photon processes were always very interesting for physicists due to the fascinating opportunity to study conversion of pure light to matter. In this paper we cover rather conservative and well-established topics of the two-photon physics, namely quarkonium spectroscopy, Higgs production, tau pair production and photon hadronic structure. All suggested measurements are aimed to improve significantly the precision of existing experiments and without any doubt are achievable under the planned characteristics of the future e^+e^- colliders. The integrated luminosity for the gamma-gamma collisions above the W^+W^- threshold (see Fig. 2, right) will be slightly less than 1 fb^{-1} which is comparable to the total e^+e^- luminosity recorded by the LEP2 experiments.

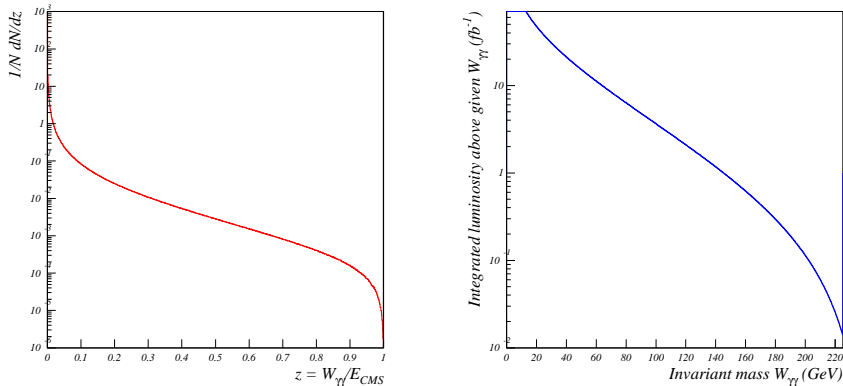


Figure 2: Left: number of $\gamma\gamma$ collisions as a function of the $\gamma\gamma$ invariant mass relative to the e^+e^- CMS energy. Right: integrated luminosity of the $\gamma\gamma$ collisions above certain collision energy, under the assumption of 5.6 ab^{-1} integrated luminosity of e^+e^- collisions.

3 Quarkonium spectroscopy

Quarkonium is regarded as the simple hadronic systems to explore the QCD aspects at the low energy regimes through its spectroscopy [14].

Quarkonia, the bound states of a heavy quark c , b and the corresponding anti-quark, can be most effectively studied at e^+e^- colliders. Since the discovery of the J/ψ in 1974, a lot of information about bounded $b\bar{b}$ and $c\bar{c}$ states was elaborated.

Quarkonium can be described as bound quark-antiquark state, with Coulombic short-distance potential with logarithmic modification of coupling strength and linear long-distance potential for quark confinement description [14],[15].

Although there exist a lot of different ways to quantitatively describe quarkonia, e.g. Lattice QCD [16], NRQCD methods [17], Light front quark model[18] or exotic like instanton liquid model [19], there are still many inconsistencies between predicted and measured radial excitation mass spectra of quarkonium states.

Due to negative charge parity of the photon, only neutral particles with even charge conjugation $C = 1$ can be produced in the two-photon collisions. There is a lot of interesting tasks concerning light mesons constituted from light u, d quarks, e.g. π, η, η' and their excited states, but we expect that CEPC experiments will be insensitive to the hadronic systems with masses below 3 GeV due to the issues of detector resolution and experimental environment. Therefore the most straightforward studies can be done with heavy c and b quarks, which lead us to the charmonia and bottomonia spectroscopy.

Charmonium states with even charge conjugation $C = 1$ up to the $\eta_c(2S)$ mass of 3637 GeV are well studied, their radiative decays to photons have been seen and measured. χ_{c1} production in two-photon collision was recently seen by BELLE collaboration [20]. However, only upper limit on branching ratio is available so far (see Table 1). From numerical estimation of event number (see Sect. 3.2, double

fraction	η_c	χ_{c_0}	χ_{c_1}	χ_{c_2}	$\eta_c(2S)$
10^{-4}	1.57 ± 0.12	2.04 ± 0.09	$< 6.3 \times 10^{-2}$	2.85 ± 0.1	1.9 ± 1.3

Table 1: Charmonium low state radiative decay branching ratio

tag set-ups) we can conclude that it is definitely possible to improve accuracy of $\gamma\gamma$ branching ratio for χ_{c_1} and $\eta_c(2S)$ charmonium states, and to measure at least the Q^2 dependence of resonance formation in single-tag set-up, where we expect approximately 10^4 events for each charmonium state.

The event yield estimation of charmonium production with the mass larger than that of $\eta_c(2S)$ is more tricky. From one point of view the $c\bar{c}$ spectroscopy at that region of mass states is very interesting due to lack of knowledge about internal structure and branching ratio to two photons of resonances (see Table 2), so any results on measurement or lower limit estimation of $\gamma\gamma$ width are highly appreciated. Moreover, the measurement of Q^2 dependence of resonance formation could give us hard restriction over quantum numbers and internal structure of resonances under consideration.

The charmonium bound states with masses above open charm threshold can not be described only in the frames of constituent quark model that describes the observed meson spectrum as $q\bar{q}$ bound states (see Table 2). To explain unexpected quantum numbers, masses, branching ratios and other properties of the heavy resonances that form the charmonium spectrum, various possibilities of new physics states are considered: meson states that are made of bound gluons (glueballs), qq-pairs with an excited gluon (hybrids), multi-quark color singlet states such as qq $\bar{q}\bar{q}$ (tetraquarks) and molecular bound states of 4-quark system, six-quark and 'baryonium' bound states.

The other side of the problem is that without a knowledge of the internal structure it is not possible to make a firm estimation of the charmonium state production. Even a naive equivalent photon approximation with narrow resonance approximation is not applicable due to unknown branching ratio to two photons.

A rough estimation of production rate we suggest to make under assumption that all charmonium states mostly consist of $c\bar{c}$ states. We know that branching ratio of the two photon quarkonium decay at lowest order does not depend on the state mass and has slight (up to a factor of few) dependence on its quantum numbers (see [21] and Table 1). So two photon branching ratio could be estimated at the level of 10^{-4} . That estimation gives us about $10^7 - 10^8$ events in no-tag mode (although we do not observe scattered leptons, it is possible to reduce background events by imposing a strict transverse-momentum balance along the beam axis for the final-state hadronic system [22]), and about 10^4 events in single (minimal angle of detection at 6 degrees) and double tag (using the luminosity calorimeter) modes. All estimations are made with accelerator parameters described in Sect. 3.2. For the estimations with no-tag mode the events with scattered electrons were also

accepted, with negligible contribution to the total event yield.

As a result we can conclude that if the recently discovered charmonium resonances (Table 2) are similar to the charm quark bound state, we should definitely discover their quantum numbers and measure the two photon branching ratios.

name	J^{PC}	Width (MeV)	$\Gamma_{\gamma\gamma}$	nature
$\chi_{c0}(3860)$	0^{++}	201 ± 101	seen	$c\bar{c}$ + possible non- $q\bar{q}$ states
$\chi_{c1}(3872)$	1^{++}	1.19 ± 0.21	seen	candidate for an exotic structure
X(3915)	0 or 2^{++}	20 ± 5	seen	$c\bar{c}$ + possible non- $q\bar{q}$ states
$\chi_{c2}(3930)$	2^{++}	24 ± 6	seen	$c\bar{c}$ + possible non- $q\bar{q}$ states
X(3940)	$???$	37 ± 17	-	$c\bar{c}$ + possible non- $q\bar{q}$ states
X(4050)	$?^{?+}$	82 ± 28	-	candidate for an exotic structure
X(4100)	$???$	152 ± 70	-	candidate for an exotic structure
$\chi_{c1}(4140)$	1^{++}	22 ± 7	not seen	candidate for an exotic structure
X(4160)	$???$	139 ± 60	-	$c\bar{c}$ + possible non- $q\bar{q}$ states
X(4250)	$?^{?+}$	177 ± 70	-	candidate for an exotic structure
$\chi_{c1}(4274)$	1^{++}	49 ± 12	-	candidate for an exotic structure
X(4350)	$?^{?+}$	13 ± 10	seen	$c\bar{c}$ + possible non- $q\bar{q}$ states
$\chi_{c0}(4500)$	0^{++}	92 ± 29	-	candidate for an exotic structure
$\chi_{c0}(4700)$	0^{++}	120 ± 50	-	candidate for an exotic structure

Table 2: Charmonium exotic states that could be seen at $\gamma\gamma$ collision

For the bottomonium states only ground state $\eta_b(9399)$ decay to two photons was seen, and other $C = +1$ states radiative decay were not measured [23], so any information about them, e.g. upper limit on the two photon branching or decay event observation, are highly appreciated.

At the Sect. 3.2 we estimate low bottomonium states $1S, 1P, 2S$. Event number of positive charge parity states with higher radial quantum number, namely $\chi_{b0}(2P)$, $\chi_{b1}(2P)$, $\chi_{b2}(2P)$, $\chi_{b1}(3P)$, $\chi_{b2}(3P)$ are estimated as counterparts with radial quantum number equal to unity.

With the number of bottomonium state events of approximately 10^5 in no-tag mode and 10^2 with double-tag we could conclude that we definitely can at least put upper limit on radiative decay branching of bottomonium states.

3.1 Theoretical estimation

We can estimate theoretically the full cross-section of two photon meson production with the help of equivalent photon approximation formula (2), where cross-section of meson with spin J, mass M photoproduction can be estimated trough:

$$\sigma_{mes}(W^2) = (2J + 1)8\pi^2 \frac{\Gamma_{\gamma\gamma}}{M} \frac{1}{\pi} \frac{M\Gamma}{(M^2 - W^2)^2 + M^2\Gamma^2}, \quad (4)$$

here $\Gamma_{\gamma\gamma}$ and Γ are the two photon and total width of meson decay.

3.2 Number of event estimation

Simulation was performed with the GALUGA [10, 11, 24], two photon production generator, where virtualities Q^2 of photons are fully taken into account through five structure functions describing photon scattering with different polarizations. Such a consideration gives one the possibility to make a robust estimation of meson production at large photon virtualities (large electron or positron scattering angle). Resonance formation in two-photon scattering are calculated in the framework of constituent-quark model [11].

The expected event yields are presented for the total beam energy $\sqrt{s} = 240$ GeV and integrated luminosity 5 ab^{-1} .

name	No Tag	S Tag 10	S Tag 6	D Tag 6	D Tag 6-1.9	D Tag 1.9-1.9
η_c	$1. \times 10^9$	5.3×10^5	1.7×10^5	7.6×10^2	1.2×10^4	8.6×10^4
χ_{c0}	$2. \times 10^8$	6.5×10^4	2.2×10^4	6.3×10^1	$9. \times 10^2$	8.3×10^3
χ_{c1}	$7. \times 10^6$	4.4×10^4	1.1×10^4	1.7×10^2	2.4×10^3	1.7×10^4
χ_{c2}	9.5×10^7	3.1×10^4	9.8×10^3	5.4×10^1	7.2×10^2	6.7×10^3
$\eta_c(2S)$	2.4×10^8	2.1×10^5	6.4×10^4	4.1×10^2	$6. \times 10^3$	4.1×10^4

Table 3: Estimation of event number for charmonium states. Single tag, no tag and double tag set-ups are considered. Cuts on electron or positron scattering angle are 1.9, 6 and 10 degrees.

Quarkonium production was estimated in three different modes, namely no tag, where no final scattered electron or positron detected (there is no limitation on the polar angle of the scattered electron/positron), single tag, where electron or positron are detected and double tag (both electron and positron are detected). The minimal angles are taken equal to 6 or 10 degrees (various detector characteristics are considered), and 1.9 degrees for the case when scattered electron or positron can be detected in the luminosity calorimeter.

From the Tables (3,4) one can see that the numbers of registered mesons are drastically dependent on the minimal angle of the scattered lepton detection. By using the luminosity calorimeter for detection of scattered leptons (the minimal detection angle of 1.9 degrees) one can enhance the statistics of registered mesons by two orders of magnitude. This emphasizes the significance low-angle calorimeter for the two-photon physics.

As one can see, in no-tag mode, where no lepton are registered at final state, we expect a large number of events, $10^7 - 10^8$ for quarkonium states and 10^5 for bottomonium. But the absence of kinematical constraints in the no-tag mode will result in huge background contamination. Some special techniques like strict transverse-momentum balance for final state could be applied to reduce background. The

name	No Tag	S Tag 10	S Tag 6	D Tag 6	D Tag 6-1.9	D Tag 1.9-1.9
$\eta_b(9399)$	1.3×10^6	1.4×10^4	3.9×10^3	1.1×10^2	$1. \times 10^3$	3.6×10^3
$\chi_{b_0}(1P)$	9.6×10^4	5.2×10^2	1.4×10^2	2.7	$3. \times 10^1$	1.5×10^2
$\chi_{b_1}(1P)$	3.9×10^3	5.1×10^2	1.3×10^2	6.6	5.3×10^1	1.4×10^2
$\chi_{b_2}(1P)$	8.3×10^4	4.9×10^2	1.2×10^2	3.4	3.4×10^1	1.6×10^2
$\eta_b(9999)$	4.6×10^5	5.8×10^3	1.6×10^3	4.9×10^1	4.4×10^2	1.5×10^3

Table 4: Estimation of event number for bottomonium states. Single tag, no tag and double tag set-ups are considered. Cuts on electron or positron scattering angle are 1.9, 6 and 10 degrees.

exact estimation of no-tag quarkonium sensitivities could be produced only with a detailed detector simulation.

For quarkonium two-photon physics on CEPC we suggest to use a conservative estimation, namely the single-tag mode (one detected lepton helps to reconstruct final state kinematics and drastically reduces the background events) and efficiency of detection about 10%. In that case we will reconstruct about $10^2 - 10^4$ events for each charmonium state. For bottomonium states we could definitely measure low-state η_b with number of registered events about 4×10^2 and possibly see some events or make upper bound for higher bottomonium states.

4 Higgs boson production

The vertex $H\gamma\gamma$ is forbidden in the SM at tree level. The decay process $H \rightarrow \gamma\gamma$ as well as the production process $\gamma\gamma \rightarrow H$ proceed mostly through the top-quark and W loops and is sensitive to contributions of new charged particles, so an observation of an excess in the $\gamma\gamma \rightarrow H$ process would indicate a new physics phenomena, e.g. a contribution of the anomalous $H\gamma\gamma$ vertex.

At e^+e^- colliders the main background to the process $\gamma\gamma \rightarrow H$ (referred as “signal” hereafter) are the Higgs boson production via the fusion of virtual Z bosons ($ZZ \rightarrow H$) and $\gamma\gamma$ collisions with final states identical to those of Higgs decays but without a formation of the intermediate Higgs boson. The background from $\gamma\gamma$ collisions can be strongly suppressed by selecting the “single-tag” events where one of the beam particles is scattered to a significant angle and is detected in the luminosity calorimeter. The signal reduction due to this selection is relatively small (by only a factor of 3 to 5) since the Higgs boson production is characterized by a large q^2 transfer. In the following we assume an event selection with a beam particle scattered by at least 30 milliradians, which is well within the acceptance of the luminosity monitor [25]. The signal and the main background sources have been simulated with PYTHIA generator [26]. No detailed detector simulation has been performed, however the main features of the proposed CEPC detector [25] have

been taken into account.

4.1 Higgs photoproduction measurement plans

Today the Higgs photoproduction at future lepton colliders attracts surprisingly low attention.

Nevertheless there was a vivid discussion in frames of Higgs boson production in ultraperipheral collisions (UPC) at LHC (proton and heavy ion collision cases was considered, see Silveira talk [27] and references therein) where estimations of Higgs photoproduction was made for different set-ups and energies.

Recently there was published a paper [28] devoted to the estimation of photoproduction of Higgs boson at the LHeC [29], proposed electron-proton collider at LHC.

Also there exist a lot of estimations and proposals to measure double Higgs photoproduction at a photon collider, particularly due to the possibility to probe trilinear Higgs interactions [30],[31].

4.2 Theoretical estimation of event number

For estimation of Higgs production rate due to two-photon mechanism we could utilize the equivalent photon approximation, elaborated in the papers [6], [32], and [9]:

$$\sigma_{ee \rightarrow eeH} \approx 2 \left(\frac{\alpha}{\pi} \right)^2 \left(\ln \frac{E}{m_e} \right)^2 \times \int_0^{4E^2} \frac{dW^2}{W^2} f\left(\frac{W}{2E}\right) \sigma_{\gamma\gamma \rightarrow H}(W),$$

here $\sigma_{\gamma\gamma \rightarrow H}(W)$ means Higgs photoproduction cross-section estimation and function f was defined in eq. (3). Here we consider only leading logarithm approximation.

The subprocess cross section for the two photon Higgs production can be calculated through narrow resonance estimation [33]:

$$\begin{aligned} \sigma_{\gamma\gamma \rightarrow H}(W) &\approx 8\pi^2 \frac{\Gamma_{\gamma\gamma}}{M_H} \frac{1}{\pi} \frac{M_H \Gamma}{(M_H^2 - W^2)^2 + M_H^2 \Gamma^2} \approx \\ &\approx 8\pi^2 \frac{\Gamma_{\gamma\gamma}}{M_H} \delta(W^2 - M_H^2), \end{aligned}$$

here $\Gamma_{\gamma\gamma}$ and Γ are the two photon and total width of Higgs decay correspondingly, M_H is the Higgs mass.

Given the energy of initial electron beam $E = 120$ GeV and $\Gamma_{\gamma\gamma} = 2.27 \times 10^{-3} \Gamma$, $\Gamma \approx 4.2$ MeV [23] we could roughly estimate the Higgs two photon production at CEPC energies at the level of 0.25 fb.

It is very interesting that the Higgs production rate through two photon mechanism at CEPC and LHC are comparable. In the latter case the estimation gives the cross section about 0.1 fb, see [34],[35],[36]

4.3 Background from the ZZ fusion

The energy dependencies of the signal $\gamma\gamma \rightarrow H$ and the background $ZZ \rightarrow H$ processes [26] are compared in Fig.3. One can see that at high energy colliders the $ZZ \rightarrow H$ background rate is much higher than that of the signal. However, at the e^+e^- CMS energies near 240 GeV the background drops abruptly and becomes comparable to the signal. The CEPC and FCC-ee colliders are therefore perfectly suited to study the $\gamma\gamma \rightarrow H$ process.

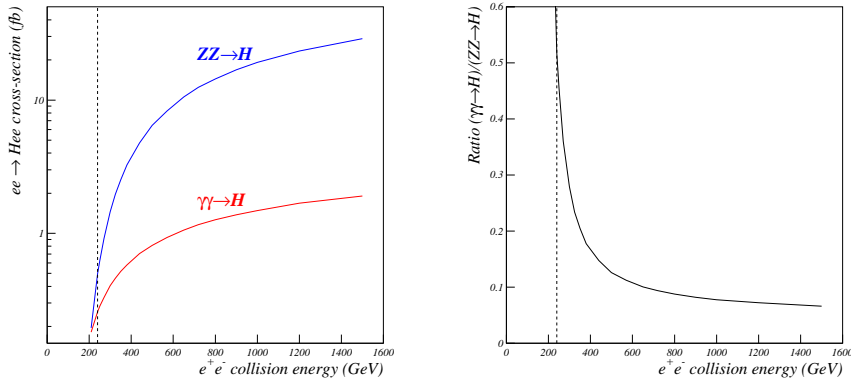


Figure 3: Left: energy dependence of $e^+e^- \rightarrow He^+e^-$ cross-section for the signal $\gamma\gamma \rightarrow H$ and background $ZZ \rightarrow H$ contributions. Right: energy dependence of the signal to background ratio. Vertical lines indicate 240 GeV CMS energy.

At 240 GeV the total signal cross-section is 0.26 fb [26], to be compared with 0.50 fb for $ZZ \rightarrow H$ background. The background can be significantly reduced using the fact that the typical q^2 transfer in the $ZZ \rightarrow H$ events is much larger than in the $\gamma\gamma \rightarrow H$ process. The distribution of the scattering angle is presented in Fig.4. Nearly all background is removed with the requirement that the beam particle is scattered by less than 24° .

Fig.5 shows the energy distribution for the scattered beam particles with the scattering angle between 30 mrad and 24° . An additional energy cut $E > 15$ GeV is applied to the scattered particle to ensure a reliable identification in the luminosity calorimeter. After the cuts on the angle and the energy of the scattered particle the cross-section is 0.049 fb for the signal and 0.027 fb for the $ZZ \rightarrow H$ background. Assuming 5.6 ab^{-1} integrated luminosity, this corresponds to 273 and 154 events, respectively.

4.4 Background from other hard processes

The Higgsstrahlung $e^+e^- \rightarrow ZH$ is the most abundant Higgs production process at 240 GeV collision energy. The “single-tag” signal can be caused by an electron from

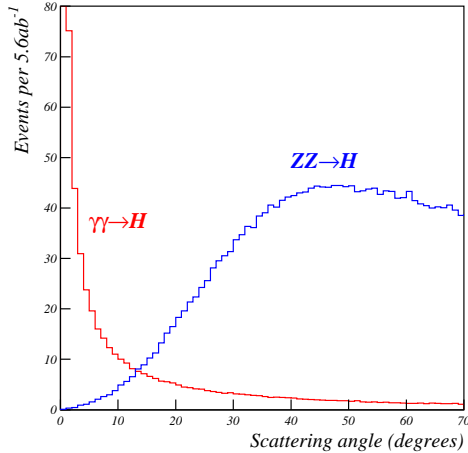


Figure 4: Distribution of the beam particle scattering angle for $\gamma\gamma \rightarrow H$ signal and $ZZ \rightarrow H$ background. The number of events is normalized to 5.6 ab^{-1} integrated luminosity.

the Z-boson decay. The cross-section of $e^+e^- \rightarrow ZH \rightarrow eeH$ is 6.7 fb. A requirement that one of the electrons is found in the “single-tag” region between 30 mrad and 24° reduces the effective cross-section to 1.4 fb. Further background reduction is achieved by the requirement that the second electron is not reconstructed in the tracker. The events with second electron outside of the tracking system (less than 10 degrees from the beam) correspond to 0.030 fb, which is similar to the background from ZZ fusion. Still this electron can be reconstructed in the luminosity calorimeter. Although the reconstruction efficiency is not perfect, the background can be reduced to a negligible level compared to ZZ fusion. The electrons outside of the luminosity calorimeter (less than 30 mrad from the beam) correspond to 0.001 fb, which is also negligible.

Another “standard” mechanism of Higgs boson production is the WW fusion $e^+e^- \rightarrow H\nu\nu$. The “single-tag” signal can be produced by an ISR photon in the angular acceptance between 30 mrad and 10° (at larger angles photons are distinguished from electrons by the tracking system). The total WW fusion cross-section is approximately 5 fb at 240 GeV. The presence of the “tag” photon reduces this to 0.032 fb, which is similar to the ZZ fusion background. Further background reduction is based on the large missing transverse momentum in $H\nu\nu$ events. A very loose cut $P_T^{miss} < 20 \text{ GeV}/c$ rejects only 4% of the signal while the WW fusion background is reduced to 0.008 fb, which is only a small fraction of the ZZ fusion background.

A W pair production is a potentially dangerous background due to its high cross-section (approximately 15 pb at 240 GeV). The “single-tag” signal can be produced by electrons from the leptonic W decays. However, this background is reduced by

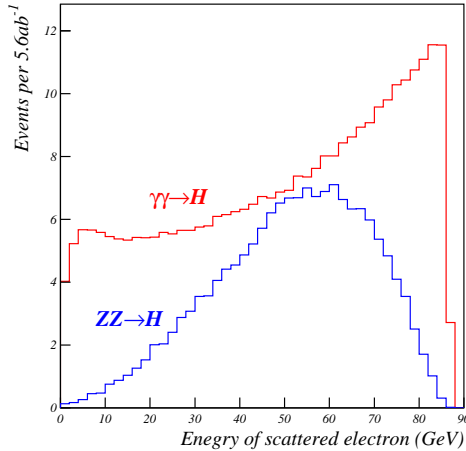


Figure 5: Energy distribution of the beam particle with scattering angle between 30 mrad and 24° for $\gamma\gamma \rightarrow H$ signal and $ZZ \rightarrow H$ background.

several very large factors: branching of $WW \rightarrow cse\nu$ decays (factor 14); probability of simultaneous fake b-tagging of both c and s quarks (factor of at least 500); electron production outside of the tracking system (factor 70); reconstruction of the hadronic W decay with a Higgs boson mass (factor of at least 20); requirement of a low P_T^{miss} (factor of 7). Taken together, the above factors reduce the $e^+e^- \rightarrow W^+W^-$ to a negligible level.

4.5 Background from non-resonant $\gamma\gamma$ collisions

The most abundant (58%) Higgs decay channel is $H \rightarrow bb$. In this channel the most significant background is the non-resonant production of b quark pairs in the $\gamma\gamma$ collisions, $\gamma\gamma \rightarrow bb$. In addition, there is a reducible background $\gamma\gamma \rightarrow cc$, where both jets from c quarks are tagged as b jets. The background from light quarks can be neglected since it is efficiently suppressed by the b -tagging.

With the “single-tag” selection described above the $\gamma\gamma \rightarrow bb$ cross-section is 94 fb for the full range of the bb invariant masses. It is reduced to 0.77 fb for $M_{bb} > 100$ GeV. According to the CEPC CDR [25], the invariant mass resolution in $H \rightarrow bb$ decays is about 5 GeV. Within the $\pm 1\sigma$ window around the Higgs mass ($120 < M_{bb} < 130$ GeV) the $\gamma\gamma \rightarrow bb$ background is 0.124 fb, more than 5 times higher than the signal (taking into account the branching fraction of the $H \rightarrow bb$ decay).

The total cross-section of the single-tag $\gamma\gamma \rightarrow cc$ production is 2086 fb. It is reduced to 13.6 fb for $M_{cc} > 100$ GeV and to 1.8 fb for $120 < M_{cc} < 130$ GeV. Although the cc background is almost 2 orders of magnitude higher than the signal,

it can be efficiently reduced by the b-tagging. According to the CEPC CDR, the c jet rejection factor is 10 for the 80% b jet efficiency. Applying the b-tagging to both jets, one gets 64% efficiency for the signal tagging and a factor of 100 reduction of the charm background, making the latter much smaller than the $\gamma\gamma \rightarrow bb$ background.

The non-resonant background can be additionally reduced using a cut on the direction of the produced b and c jets. Fig. 6 shows the distribution of the quark polar angle. The background jets are concentrated near the beam axis. We apply a polar angle cut $\Theta > 20^\circ$ for both quarks. Within this acceptance we assume (for the signal and the background) a 75% efficiency to reconstruct both jets from b or c quarks.

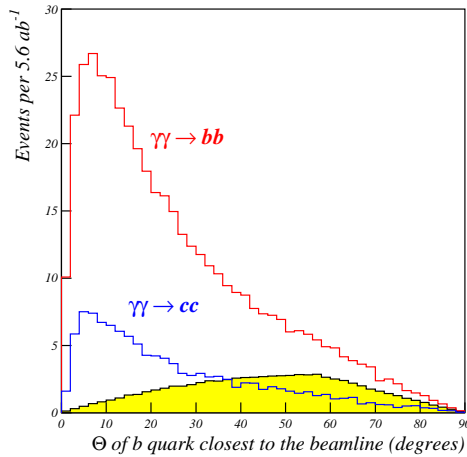


Figure 6: Distribution of the polar angle of the quark closest to the beam line. Shaded area is the $\gamma\gamma \rightarrow H$ signal, open histograms represent the non-resonant background. The events are shown within the invariant mass window $118 < M_{bb} < 132$ GeV.

The M_{bb} invariant mass distribution is presented in Fig.7. The Higgs signal is smeared assuming a 5 GeV mass resolution. Within the window 118-132 GeV the expected signal is 57 events, the peaking ZZ background is 33 events and the non-peaking background is 278 events. A fit to the signal and background yields results in about 4.1σ signal significance for the $H \rightarrow bb$ channel, after the subtraction of the $ZZ \rightarrow H$ background. The signal significance can be further improved by including other Higgs decay modes. We conclude that the $\gamma\gamma \rightarrow H$ signal can be reliably observed with the planned CEPC luminosity.

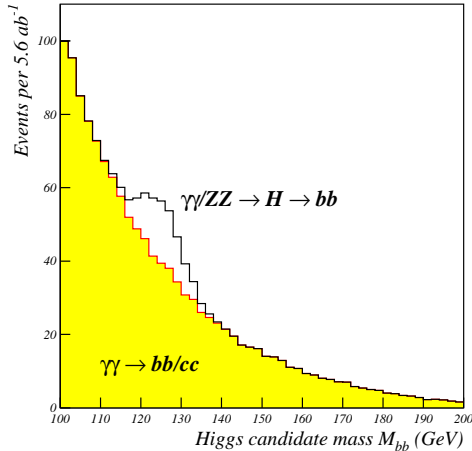


Figure 7: Distribution of the invariant masses of the Higgs candidates. Shaded area represents $\gamma\gamma \rightarrow bb/cc$ backgrounds, open histogram is the signal, with a small contribution from the $ZZ \rightarrow H$ events.

5 Tau pair production

At present, the anomalous magnetic moments of electron and muon are measured with an enormous precision, better than one per billion and one per million, respectively. These measurements provide an extremely important test of the Standard Model. At the same time, the anomalous magnetic moment of the tau lepton, a_τ , is known with rather poor accuracy.

The measurement of a_τ is interesting in two respects. First, because of the large tau mass, a_τ is sensitive to the contributions of the new physics at higher scales. Second, many theoretical models predict that the new physics effect manifest themselves only in the properties of the third-generation fermions. Thus, the overwhelming success of the Standard Model observed in the sector of anomalous magnetic moment might be just a consequence of performing the high precision measurements with the leptons of only first generations.

The most precise determination of a_τ (17 permille) was performed by the DELPHI experiment at LEP2. The total luminosity was approximately 0.5 fb^{-1} taken at the c.m.s. energies between 182 and 208 GeV. The tau anomalous magnetic moment was extracted from the absolute cross-section of the tau pair production in gamma-gamma collisions. The simplest final state was selected with one tau decaying to an electron, another to a muon. The DELPHI precision of the cross-section measurement was about 4%.

At CEPC the integrated luminosity will be increased by 4 orders of magnitude

with respect to LEP2. Thus, an improvement of a_τ precision by a large factor can be expected.

At the collision energy of 240 GeV the QED cross-section of the $e^+e^- \rightarrow e^+e^-\tau^+\tau^-$ process is 570 pb [37]. This corresponds to nearly 3 billions events with 5 ab^{-1} of integrated luminosity, or 165 millions events with the $e - \mu$ final state.

At LEP2 the selection efficiency for the $e - \mu$ final state was 15-20%. In the CEPC environment a tighter selection might be necessary to cope with the high background. We conservatively consider the following severe cuts: at least one of the two tracks must have the transverse momentum $p_T > 5 \text{ GeV}/c$, the other track must have $p_T > 3 \text{ GeV}/c$. In addition, we require that directions of the both tracks are more that 20 degrees from the beam axis, and that the total energy of the two particles is less than 30 GeV to remove the annihilation events.

Fig.8 shows the distribution of the transverse momentum of the leading and subleading tracks in the $\gamma\gamma \rightarrow \tau\tau \rightarrow e\mu$ events. One can see that only a very small fraction of the events satisfy the selection cuts. Fig.9 shows the distribution of the invariant mass of the electron and the muon after applying the selection cuts.

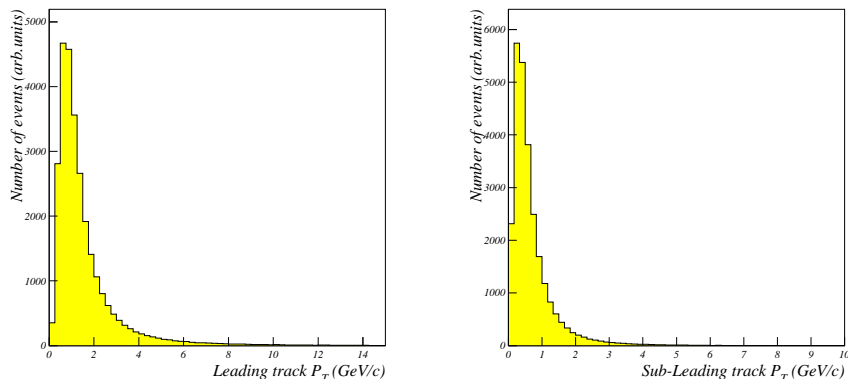


Figure 8: Distribution of the transverse momenta of the leading (left) and subleading (right) tracks in the $\gamma\gamma \rightarrow \tau\tau \rightarrow e\mu$ events.

The above selection has the generator-level efficiency of 0.42%, corresponding to the total statistics of about 700 thousands events. Thus, the statistical error is expected to be at the permille level and the measurement is likely to be systematically limited.

Given the very clean and simple final state, one can optimistically expect to keep the total systematic error at 0.5% level. This will include the absolute luminosity determination (0.1%), tracking and Particle Identification efficiency (0.15% per track for the tracking and a similar number for the PID), trigger efficiency, residual background.

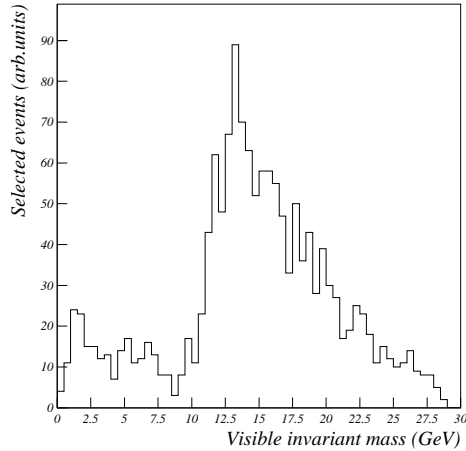


Figure 9: Distribution of the visible invariant masses of the selected $\gamma\gamma \rightarrow \tau\tau \rightarrow e\mu$ events.

With the above systematic error, the DELPHI precision can be improved by a factor of 8 for the cross-section measurement and the sensitivity to the anomalous magnetic moment would be improved by a similar factor. Adding other final states (e.g. $e-\rho$ and $\mu-\rho$) is not expected to provide a large improvement of the total error, since the measurement will be systematically dominated. However, those channels will have partially independent systematic uncertainties, providing important cross-checks and certain reduction of the overall systematic errors.

6 Photon hadronic structure

The measurement of the photon structure function (PSF) has a long history. Although the photon is considered as a point-like particle, due to the quantum effects it can fluctuate to a quark pair or a rho meson. These two processes are usually described respectively as point-like and hadron contribution to the photon structure function. The latter could be estimated in the framework of vector meson dominance model [32] while the former was calculated within quark model in leading order QCD corrections [38] and later in series of papers at NLO [39],[40] and NNLO accuracy [41].

The most recent measurements of PSF have been performed at LEP about 20 years ago, and since then publications are scarce, the most novel review of state-of-the-art could be find at [42],[43],[44].

The photon hadronic structure can be tested via the measurement of in-

clusive hadron production in gamma-gamma collisions $e^+e^- \rightarrow e^+e^-\gamma\gamma^* \rightarrow e^+e^- + \text{hadrons}$. The high-virtuality photon γ^* is radiated off an electron which scatters at relatively large angle and can be detected in the experimental setup (“tagged electron”). The second electron is usually scattered at a very small angle and thus remain undetected (“untagged electron”). The photon γ radiated by the untagged electron can be considered as quasi-real.

The overall reaction can be described as a deep inelastic scattering (DIS) $e\gamma$ of the tagged electron on the real photon. In such a scattering the hadronic nature of the target photon is effectively revealed.

Pioneering experiment of PSF F_2 measurement was done at DESY by PLUTO collaboration in 1981 [45], within the range $Q^2 \in (1, 15) \text{ GeV}^2$ at an average beam energy of 15.5 GeV. Since then many experiments made contributions so the Q^2 range was enlarged up to 780GeV^2 at PLUTO [46],[47], ALEPH [48],[49] AMY [50],[51], DELPHI [52],[53], JADE [54], L3 [55],[56] , OPAL [57], TASSO [58], TOPAZ [59], TCP/ 2γ [60].

The most recent experiments have been done at LEP by collaborations ALEPH, L3 and OPAL with similar characteristics: center of mass energy $\approx 200 \text{ GeV}$, integrated luminosity $\approx 600 \text{ pb}^{-1}$ while the minimum angle for detection in the luminosity calorimeter was 0.024, 0.03 and 0.033 rad correspondingly. Comparing this data with similar CEPC parameters, namely c.m.s. energy 240 GeV, integrated luminosity 5 ab^{-1} and minimal detection angle of about 1.9 degree (0.03 rad) one can naively estimate the number of events at CEPC to be about 10^4 times bigger than that at LEP.

The hadronic photon structure function $F_2^\gamma(x, Q^2)$ can be extracted from the differential cross-section $d\sigma/dQ^2 dx dy$, where Q^2 is the virtuality of γ^* and x, y are the Bjorken scaling variables.

For the case of single-tagged events, when one of the photon is almost real (photon invariant mass $P \approx 0$), the general process cross-section $e^+e^- \rightarrow e^+e^-\gamma\gamma \rightarrow e^+e^-X$

$$\frac{d\sigma(ee \rightarrow eeX)}{dx dz dQ^2 dP^2} = f_{\gamma/e} \frac{d\sigma(e\gamma \rightarrow eX)}{dx dQ^2}, \quad (5)$$

are factorized into almost real photon luminosity function $f_{\gamma/e}$

$$f_{\gamma/e} = \frac{\alpha}{2\pi} \left(\frac{1 + (1 - z^2)}{z} \frac{1}{P^2} - \frac{2m_e^2 z}{P^4} \right), \quad z = E_\gamma/E_{beam} \quad (6)$$

and deep inelastic proton-electron scattering cross-section [32]

$$\frac{d\sigma(e\gamma \rightarrow eX)}{dx dQ^2} = \frac{2\pi\alpha^2}{xQ^4} ((1 + (1 - y)^2)F_2^\gamma - y^2 F_L^\gamma). \quad (7)$$

Neglecting the virtuality of the quasi-real photon, one has: $Q^2 = 2E_{beam}E_{tag}(1 - \cos\theta_{tag})$, $x = Q^2/(Q^2 + W^2)$, $y = 1 - (1 + \cos\theta_{tag})E_{tag}/(2E_{beam})$, where W is the $\gamma\gamma^*$ invariant mass which is experimentally measured as the mass of the hadronic system, θ_{tag} and E_{tag} are scattering angle and energy of the tagged lepton.

Usually the experimentally accessible kinematic region corresponds to small values of y ($y^2 \ll 1$), so the contribution of the term proportional to the longitudinal structure function F_L^γ is negligible, and one can determine PSF F_2^γ directly from the cross-section (7).

The measurement of the energy E_{tag} and the polar angle θ_{tag} of the scattered electron is straightforward. The most difficult part of the analysis is the reconstruction of the hadronic invariant mass W . In addition to the finite detector resolution and efficiency, the W reconstruction is also affected by the acceptance issue, since the hadronic system is typically boosted along the beam axis and part of it remains undetected or poorly reconstructed. A sophisticated unfolding procedure is required to convert the measured visible invariant mass into the true one. An additional difficulty will be the background from overlapping interaction. This background has little impact on the hard processes, but must be carefully taken into account in the studies of gamma-gamma collisions.

The scattered electron can be reconstructed either in the luminosity monitor (probing the small Q^2 values with high statistics), or in the forward electromagnetic calorimeter. In the latter case the domain of high Q^2 values can be accessed. The available range of very high Q^2 is limited by the low statistics due to the steeply falling spectrum of scattering angles. Given the unprecedented luminosity, the future e^+e^- colliders will be able to study the photon structure function in the high Q^2 domain which was never accessed by other experiments.

At LEP2 the explored range of Q^2 was limited to about 10^3 GeV², mainly due to the available statistics. At CEPC the collision energy will be comparable to LEP2. However, the huge statistics expected at the future colliders (several orders of magnitude increase) allows one to explore the kinematical regions that could not be accessed by the past experiments due to the limited statistics. Among them, the following can be mentioned:

- Measurement of the photon structure function at the very high virtualities Q^2 , corresponding to the very large electron scattering angles.
- Double-tagged events, where both beam particles are detected. In this situation the whole event is fully reconstructed, which will dramatically reduce the systematic uncertainty at the expense of the low available statistics.

This case of deeply virtual target photons $Q^2 \gg P^2 \gg \Lambda_{QCD}$ is very interesting because it is purely perturbative and allows one to compare the experimental values with absolute QCD predictions.

7 Conclusions

In this paper we study several interesting topics of two-photon physics that could be considered at future electron-positron colliders, CEPC and FCC-ee. As a reference we take the planned CEPC set-up with c.m.s. energy $\sqrt{s} = 240$ GeV, integrated luminosity 5.6 ab⁻¹ and assume that a forward electromagnetic calorimeter will

cover the polar angles down to 1.9 degrees. Our qualitative results can be applied to FCC-ee project, taking into account its similar expected performance.

We have considered a rather limited set of topics of two-photon physics, namely quarkonium spectroscopy, Higgs and tau pair production, photon hadronic structure. Our estimations are based on a conservative approach and without any doubt the quantitative characteristics can be surpassed in the real experiments. New physics problems like searching for MSSM heavy Higgs, anomalous top quark interactions, new physics state searching will be considered elsewhere.

In Sect. 3 we consider quarkonium two-photon physics in three possible detection modes: no-tag, single- and double tag. We show that using low-angle calorimeter (1.9 degree minimal detection angle) could drastically improve statistics of tagged events by two orders of magnitude. In no-tag mode we expect about 10^7 - 10^8 quarkonium and 10^5 bottomonium events. Taking into account the efficiency of detection about 10% and considering single-tag mode for better reconstruction of final state and reducing background events, we estimate about $10^2 - 10^4$ registered events for charmonium states. For bottomonium we could expect about 4×10^2 of low-state η_b and possibly see some events or make upper bound for higher states.

We find (Sect. 4) that photoproduction of Higgs can be observed with total cross-section about 0.25 fb and luminosity of collider $5.6 ab^{-1}$. Possible background issues from non-resonant $\gamma\gamma$ collisions and $ZZ \rightarrow H$ were discussed and it was shown that by choosing appropriate selection cuts one could achieve more than 4σ signal significance for the $H \rightarrow bb$ channel.

The tau pair production cross-section and anomalous magnetic moment measurement can be improved up to a factor 8 compared with the precision of DELPHI experiment at LEP (Sect. 5).

Statistical error of photon structure function measurement (Sect. 6) could be improved by about two orders of magnitude compared to the LEP experiments. Also we expect that due to the high luminosity of the future colliders it will be possible to perform measurements of PSF at very high virtualities Q^2 .

More detailed analysis and thorough simulation of events, background, systematic and statistical errors of physical quantities to measure can be estimated after exact characteristics of planned colliders and detectors will be known.

8 Acknowledgements

Authors are grateful to prof. Li Haibo for fruitful discussions which inspired this work. The work of V.V.B. was supported in part by the Heisenberg-Landau Program.

References

- [1] “A Multi-TeV Linear Collider Based on CLIC Technology: CLIC Conceptual Design Report”, CERN report CERN-2012-007, Geneva, 2012.
- [2] “The International Linear Collider Technical Design Report”, ILC report ILC-REPORT-2013-040, 2013.
- [3] “CEPC Conceptual Design Report. Volume I - Accelerator”, IHEP report IHEP-CEPC-DR-2018-01, 2018.
- [4] “FCC-ee: The Lepton Collider”, Eur. Phys. J. Special Topics 228 (2019) 261
- [5] V. Balakin, A. Bukin, E. Pakhtusova, V. Sidorov and A. Khabakhpashev, Phys. Lett. B **34** (1971), 663-664
- [6] F. E. Low, Phys. Rev. **120** (1960) 582.
- [7] F. Calogero and C. Zemach, Phys. Rev. **120** (1960), 1860-1866
- [8] I. F. Ginzburg, [arXiv:1508.06581 [hep-ph]].
- [9] V. M. Budnev, I. F. Ginzburg, G. V. Meledin and V. G. Serbo, Phys. Rept. **15** (1974) 181.
- [10] G. A. Schuler, Comput. Phys. Commun. **108** (1998) 279
- [11] G. A. Schuler, F. A. Berends and R. van Gulik, Nucl. Phys. B **523** (1998) 423
- [12] S. J. Brodsky, T. Kinoshita and H. Terazawa, Phys. Rev. Lett. **25** (1970) 972.
- [13] G. Abrams *et al.*, Phys. Rev. Lett. **43** (1979), 477
- [14] E. Eichten, K. Gottfried, T. Kinoshita, K. D. Lane and T. M. Yan, Phys. Rev. D **17** (1978) 3090 Erratum: [Phys. Rev. D **21** (1980) 313].
- [15] E. Eichten, S. Godfrey, H. Mahlke and J. L. Rosner, Rev. Mod. Phys. **80** (2008) 1161
- [16] H. Na *et al.*, Phys. Rev. D **86** (2012) 034506
- [17] N. Brambilla, A. Pineda, J. Soto and A. Vairo, Nucl. Phys. B **566** (2000) 275
- [18] H. M. Choi, Phys. Rev. D **75** (2007) 073016
- [19] B. Pandya, M. Shah and P. C. Vinodkumar, arXiv:1910.06111 [hep-ph].
- [20] Y. Teramoto *et al.* [Belle], Phys. Rev. Lett. **126** (2021) no.12, 122001
- [21] W. Kwong, P. B. Mackenzie, R. Rosenfeld and J. L. Rosner, Phys. Rev. D **37** (1988) 3210.
- [22] S. Uehara *et al.* [Belle Collaboration], Eur. Phys. J. C **53** (2008) 1
- [23] M. Tanabashi *et al.* [Particle Data Group], Phys. Rev. D **98** (2018) no.3, 030001.
- [24] G. A. Schuler, “Improving the equivalent-photon approximation in electron-positron collisions”, arXiv:hep-ph/9610406

- [25] CEPC Study Group, “CEPC Conceptual Design Report: Volume 2”, arXiv:1811.10545 [hep-ex].
- [26] T. Sjöstrand, S. Mrenna, and P. Skands, JHEP05 (2006) 026; Comput. Phys. Comm. 178, 852 (2008).
- [27] M. B. G. Ducati and G. G. Silveira, AIP Conf. Proc. **1350** (2011) no.1, 132
- [28] R. Li, X. Lv, B. W. Wang, K. Wang and T. Xu, arXiv:1906.08969 [hep-ph].
- [29] J. L. Abelleira Fernandez *et al.* [LHeC Study Group], J. Phys. G **39** (2012) 075001
- [30] T. Takahashi *et al.*, arXiv:0902.3377 [hep-ex].
- [31] R. Belusevic and G. Jikia, Phys. Rev. D **70** (2004) 073017
- [32] S. J. Brodsky, T. Kinoshita and H. Terazawa, Phys. Rev. D **4** (1971) 1532.
- [33] L. S. Brown, Quantum Field Theory, Cambridge University Press, 1992
- [34] V. A. Khoze, A. D. Martin and M. G. Ryskin, Eur. Phys. J. C **23** (2002) 311
- [35] E. Levin and J. Miller, arXiv:0801.3593 [hep-ph].
- [36] D. d’Enterria and J. P. Lansberg, Phys. Rev. D **81** (2010) 014004
- [37] F. A. Berends, P. H. Daverveldt, R. Kleiss, Comp. Phys. Comm. **40** (1986) 271
- [38] E. Witten, Nucl. Phys. B **120** (1977) 189.
- [39] W. A. Bardeen and A. J. Buras, Phys. Rev. D **20** (1979) 166 Erratum: [Phys. Rev. D **21** (1980) 2041].
- [40] D. W. Duke and J. F. Owens, Phys. Rev. D **22** (1980) 2280.
- [41] T. Ueda, K. Sasaki and T. Uematsu, Phys. Rev. D **75** (2007) 114009
- [42] C. Berger, J. Mod. Phys. **6** 1023
- [43] I. Schienbein, Annals Phys. **301** (2002) 128
- [44] K. Sasaki, T. Ueda and T. Uematsu, CERN Proc. **1** (2018) 7.
- [45] C. Berger *et al.* [PLUTO Collaboration], Phys. Lett. **107B** (1981) 168.
- [46] C. Berger *et al.* [PLUTO Collaboration], Phys. Lett. **142B** (1984) 111.
- [47] C. Berger *et al.* [PLUTO Collaboration], Z. Phys. C **33** (1987) 351.
- [48] R. Barate *et al.* [ALEPH Collaboration], Phys. Lett. B **458** (1999) 152.
- [49] A. Heister *et al.* [ALEPH Collaboration], Eur. Phys. J. C **30** (2003) 145.
- [50] T. Kojima *et al.* [AMY Collaboration], Phys. Lett. B **400** (1997) 395.
- [51] S. K. Sahu *et al.* [AMY Collaboration], Phys. Lett. B **346** (1995) 208.
- [52] W. Da Silva *et al.* [DELPHI Collaboration], Nucl. Phys. Proc. Suppl. **82** (2000) 43.
- [53] P. Abreu *et al.* [DELPHI Collaboration], Z. Phys. C **69** (1996) 223.

- [54] W. Bartel *et al.* [JADE Collaboration], *Z. Phys. C* **24** (1984) 231.
- [55] P. Achard *et al.* [L3 Collaboration], *Phys. Lett. B* **622** (2005) 249
- [56] M. Acciarri *et al.* [L3 Collaboration], *Phys. Lett. B* **436** (1998) 403.
- [57] G. Abbiendi *et al.* [OPAL Collaboration], *Phys. Lett. B* **533** (2002) 207
- [58] M. Althoff *et al.* [TASSO Collaboration], *Z. Phys. C* **31** (1986) 527.
- [59] K. Muramatsu *et al.* [TOPAZ Collaboration], *Phys. Lett. B* **332** (1994) 477.
- [60] H. Aihara *et al.* [TPC/Two Gamma Collaboration], *Z. Phys. C* **34** (1987) 1.